URSI GASS 2020, Rome, Italy, 29 August - 5 September 2020

Design of a Wide Dynamic Range Rectifier Array Based on Adaptive Input-Power Distribution

Pengde Wu(1), Zhongqi He*(1), and Bifeng Yang(2)
(1) Sichuan University, Chengdu, China, 610065, pengdewu2018@gmail.com
(2) Chengdu University of Information Technology, Chengdu, China, 610225, ybfjs@cuit.edu.cn

Abstract

A microwave rectifier array using adaptive input power distribution technique (AIPDT) is proposed to achieve high conversion efficiency over a wide dynamic input power range. The rectifier array employs two rectifier cells operating at low and high-power levels respectively, and utilizes AIPDT to distribute the RF input power between them according to the input power level. In this way, a high RF-DC power conversion efficiency (PCE) and a low reflection coefficient over a wide input power range are achieved. For validation, the proposed rectifier array at 2.4 GHz was designed, fabricated and characterized. The experimental results show that the PCE maintains over 50% when the input power ranges from 2.2 to 26.5 dBm, and the input power range for PCE>30% is from -7 to 30 dBm. Besides, the reflection coefficient remains less than -10 dB over 40 dB dynamic range (-10 to 30 dBm).

1 Introduction

Wireless power transfer (WPT) and wireless energy harvesting (WEH) are promising microwave/RF technologies that are capable of extending the battery life of a wireless sensor and making battery-free devices possible. One of the key components to build WPT/WEH is the rectifier with high RF-DC power conversion efficiency (PCE). However, the input power level of a rectifier may change with the distance from the RF source, the antenna orientation, and the time of day. The problem is even worse in a WEH system where the power level of the harvested RF power is not predictable. The reflection coefficient and PCE of a rectifier are functions of the input power, and thus the fluctuating input power level will cause input impedance mismatch, resulting in severe drop of PCE.

In recent years, different approaches have been explored to improve the dynamic range of a rectifier. In terms of reducing the variation of input impedance with a varying input power level, the concept of resistance compression network (RCN) has been previously introduced in [1]-[2]. Beyond the RCN, the maximum power point tracking method (MPPT), based on the closed-loop tracking and DC/DC converter, can maximize the conversion efficiency by terminating a rectifier with an optimum load, resulting in a stable efficiency over a wide input power range. As reported in [3], better matching is realized and the efficiency is improved by 10% at a relatively lower input power level. Alternatively, a power management unit (PMU) consisting of a star-up circuit and a boost converter allows the system to operate with a significantly lower input power [4]. Nonetheless, the intrinsic power consumption of the MPPT/PMU causes an efficiency dilemma when the RF input power or the harvested power is relatively low (e.g.,$\sim$10 μW-$\sim$100 mW).

An amplifier with the Doherty configuration could achieve high-power efficiency and high linearity over a wide range of output power levels [5]. Following this concept, a rectifier topology which can switch between low-power and high-power operation can effectively widen the dynamic range of the rectifier. In accordance with this idea, a high-power rectifier and a low-power rectifier are employed to extend the input power range, and the adaptive input-power distribution between the two sub-rectifiers can be achieved by RF switch [6], coupler [7]-[8], circulator [9]-[10], or power divider [11]-[12]. However, the insertion loss of the additional circuit component is unavoidable, resulting in a deterioration of PCE. For instance, in [7] and [8], the high-power and low-power branch are connected by a $\lambda/4$ branch-line coupler, so that the injected power can be optimally delivered to the sub-rectifiers. Nevertheless, the series and shunt arms of this $\lambda/4$ coupler have a total physical length of 17 mm at 2.4 GHz, which introduces an insertion loss of around 0.3 dB.

On top of those, efforts have been expended on the elimination of the circuit components between the two sub-rectifiers, such as the adaptive power distribution approach proposed in [13] and [14]. In those two works, all sub-rectifier cells share one DC load, such that the rectifying diodes are reverse biased by the same DC output voltage. However, the overall input power range is undermined by the low-power cell where a rectifying diode with low-breakdown capability is used. In addition to this, a cooperative structure using two diodes with diverse characteristics is proposed to extend the input power range [15]. It is noted that the additional diode on the signal flow-path will introduce insertion loss, resulting in a detraction of conversion efficiency.

Besides, to maintain high and stable efficiency on a wide input power range, a control circuit which can sense the

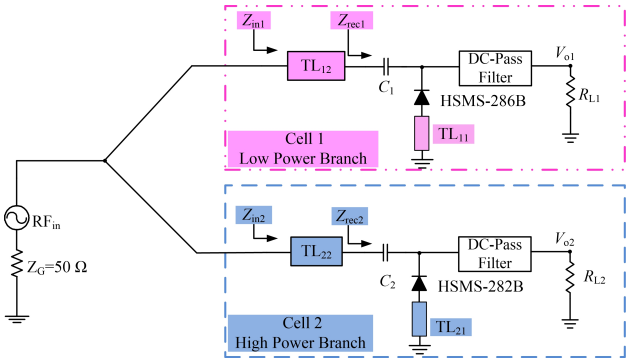

Figure 1. The schematic diagram of the proposed rectifier array with adaptive input power distribution technique (AIPDT).

input power level and adaptively switch the rectifier between different operating modes is reported in [16]. Soon afterward, to eliminate the control and sensing circuit, the pHEMT/MOSFET is utilized as an adaptive switch which can adaptively extend the breakdown voltage of the rectifying diode, and thus a wide input power range is achieved with a simple structure [17]-[18]. However, the operating frequency range of the rectifier is limited by the introduced circuit components.

Different from the previous works employing the Doherty configuration through a circulator or branch-line coupler [7]-[12], the proposed AIPDT positively increases the proportion of RF input power distributed to the high-power rectifier with the increase of input power, while decreasing that to the low-power rectifier, and vice versa. Meanwhile, the proposed AIPDT has a low-loss because it only employs two segments of microstrip-line, no complex matching network is bridged between the two rectifier cells, enabling the rectifier array to be achieved within a compact circuit area and a low insertion loss. As a result, a high PCE can be achieved over a wide input power range.

2 Design and Simulation

Fig. 1 shows the simplified schematic of the proposed rectifier array with AIPDT. It consists of two different rectifier cells which are directly connected to the input port without any additional circuits. The low-power branch, Cell 1, and high-power branch, Cell 2, are optimized for their corresponding operational regime, respectively.

As shown in Fig. 1, for each branch, a short-circuited stub TL_{n1} is applied to cancel the imaginary part of the impedance of the rectifying diode. Within the input power range of interest, a segment of transmission line TL_{n2} is further introduced to transform the complex input impedance Z_{rec1} or Z_{rec2} into a real impedance, and the input impedances after this modulation are denoted as Z_{in1} and Z_{in2}. Besides, with proper electrical lengths of TL_{n2}, Z_{in1} and Z_{in2} could inversely change with the input power, which is the key to the proposed AIPDT.

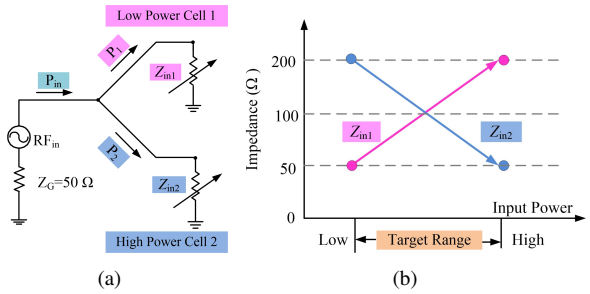

Figure 2. (a) The working principle of the proposed AIPDT. (b) The desired input impedance Z_{in1} and Z_{in2} versus input power.

2.1 Working Principle of the AIPDT

The working principle of the proposed rectifier array is indicated in Fig. 2(a) where the AIPDT is realized through the impedance variation of the two cells. As shown in Fig. 2(a), the input power of the rectifier array is denoted as P_{in}, and the real power delivered to the individual rectifier are denoted as P_{in1} and P_{in2}. As the voltages on the input impedance Z_{in1} and Z_{in2} are equal, the power distribution ratio between the cells, P_{in1}/P_{in2}, is inversely proportional to that between the rectifier cells' input impedances, which can be described as

$$\frac{P_{in1}}{P_{in2}} = \frac{Z_{in2}(P_{in})}{Z_{in1}(P_{in})} \tag{1}$$

Besides, the input impedance of the rectifier array Z_{in} is also a function of $Z_{in1,2}$. Thus, the AIPDT can be fully realized once the input matching is achieved with

$$Z_{in} = Z_{in1} || Z_{in2} = Z_G \tag{2}$$

To avoid the input power saturation of the low-power Cell 1, increasing amount of RF input power should be delivered to Cell 2 as the input power rises. Thus, from (1) and (2), the two rectifier cells are designed such that $Z_{in1,2}$ vary inversely with the input power, which is shown in Fig. 2(b). Besides, in order to extend the dynamic input power range without sacrificing the PCE, the low-power Cell 1 should be deactivated at high power level, and vice versa for the high-power Cell 2.

2.2 Simulation Results

The operating frequency of the proposed rectifier array is set to be 2.4 GHz. The input impedance $Z_{in1,2}$ are simulated in Advanced designed system (ADS, Keysight) based on a nonlinear SPICE model, and the results are shown in Fig. 3. It is observed that both Z_{in1} and Z_{in2} are real impedance from 0 to 10 dBm, and Z_{in1} increases with the input power, whereas Z_{in2} decreases with the input power. In addition, good input matching has been achieved with the proposed rectifier array ($Z_{in1}||Z_{in2}$), such that the input reflection coefficient magnitude is well below -10 dB at all the input power levels.

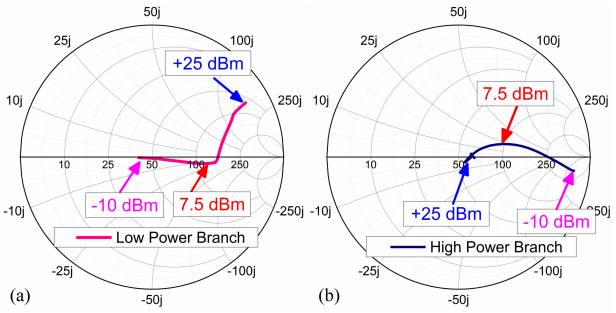

Figure 3. Simulated input impedance of a single rectifier cell from -10 to 25 dBm at 2.4 GHz. (a) Z_{in1} of Cell 1 with the low-power branch. (b) Z_{in2} of Cell 2 with the high-power branch.

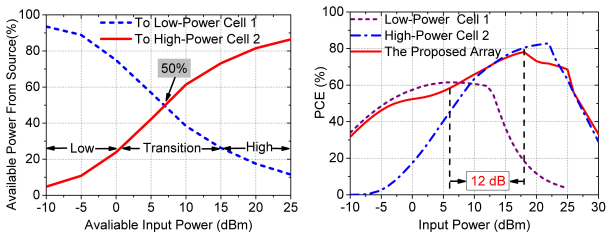

Figure 4. (a) The input power distribution between Cell 1 and Cell 2 by the power-dependant impedance $Z_{in1,2}$. (b) Comparison of the simulated PCE: Cell 1 of the low-power branch; Cell 2 of the high-power branch; the proposed rectifier array with AIPDT.

Fig. 4(a) shows the simulated power distribution between Cell 1 and Cell 2 versus input power. It can be seen that increasing amount of input power is delivered to Cell 2, with the power distribution P_{in1}/P_{in} declines as the input power P_{in} increases and P_{in2}/P_{in} rises steadily. At a lower input power, the proposed AIPDT delivers a large proportion of the input power P_{in} to the low-power branch Cell 1. For instance, at -10 dBm, the Cell 1 occupies 93.5% of the input power, the Cell 2 only makes up 6.5%, so that Cell 2 is considered to be effectively OFF. On the other hand, most of the RF power is delivered to Cell 2 in the high power region. At 20 dBm input power, the Cell 2 takes up 81.5% while the Cell 1 accounts for 17.5% of the input power .

Fig. 4(b) shows the simulated PCE of the rectifier array as compared to two individual rectifiers. The PCE of the proposed rectifier array follows the solid red line. Comparing this red line with the purple dash line of Cell 1, we can find that almost all the input power is distributed to Cell 1 within the input power range from -10 to -2 dBm. Thus, the PCE of the rectifier array is approximately equal to the PCE of Cell 1 in this region. Along the increase of the input power, Cell 2 accounts for a growing amount of the RF input power through the proposed AIPDT. Due to the relative low PCE of Cell 2 at a lower input power level (blue dash dot line), the red solid line has a slight drop between -2 to 7.5 dBm. With the continuous increase of the input power, both rectifying diodes will reach their breakdown regions. As labelled in Fig. 4(b), with the functions of the proposed AIPDT and Cell 2, the saturation point of Cell 1 has been successfully extended from 6 dBm to 18 dBm, which demonstrates an improvement of 12 dB dynamic range.

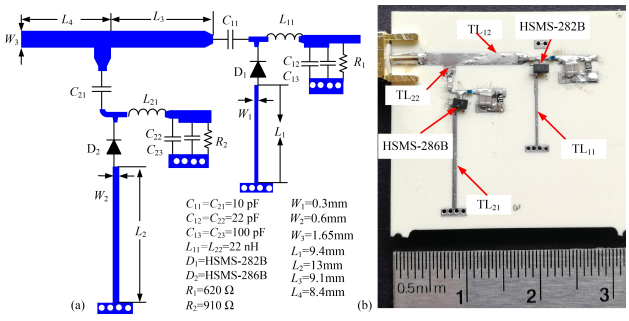

Figure 5. The proposed rectifier array with AIPDT. (a) The layout. (b) A photograph of the fabricated rectifier array.

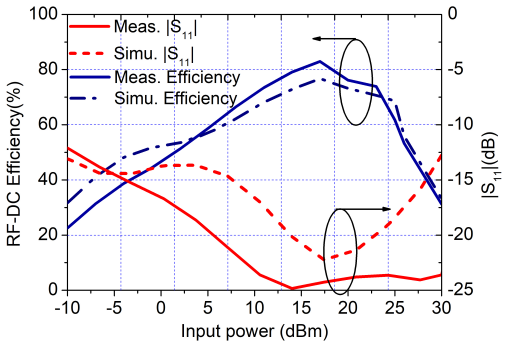

Figure 6. Measured PCE and $|S_{11}|$ versus the input power at 2.4 GHz, in comparison to simulation results.

3 Implementation and Experimental Results

The proposed rectifier was fabricated and tested. The layout of the proposed design is shown in Fig. 5(a). Rogers 4350B ($\varepsilon_r = 3.66$ and $\tan\delta = 0.002$) was used as the substrate, Fig. 5(b) shows a photo of the prototype rectifier. As can be seen, complex matching circuits and impedance transformation are not used in the proposed structure, leading to a simple structure. The measured PCE can be calculated with

$$\eta_{PCE} = \frac{P_{\text{Low}} + P_{\text{High}}}{P_{in}} \times 100\% \qquad (3)$$

where P_{Low} and P_{High} are the output DC power of the two rectifier cells, and P_{in} is the RF input power of the proposed rectifier array.

Fig. 6 depicts the measured and simulated PCE versus input power at 2.4 GHz. As observed, the measured PCE remains more than 50% within the input power range from 2.2 to 26.5 dBm. In addition, the proposed design demonstrates $>30\%$ PCE over a range of 37 dB input power level (-7 to 30 dBm). The maximum measured PCE of the proposed rectifier is 81.9% at 17 dBm. Furthermore, the measured $|S_{11}|$ is well below -10 dB within the whole input range, such that a dynamic range of 40 dB for $|S_{11}| < -10$ dB can

be achieved. There are still some discrepancies between the measurements and simulations, which are due to the inaccurate diode models and fabrication errors.

4 Conclusion

In this letter, an adaptive input power distribution technique (AIPDT) has been presented to facilitate the design of a rectifier array which can achieve high conversion efficiency over a wide input power range. By using AIDPT, the input impedance variations of the two rectifier cells are neutralized, so that the proposed rectifier array has achieved good input impedance matching over a wide input power range, resulting in a dynamic range of 40 dB for $|S_{11}|$ <-10 dB.

References

[1] C. Song, Y. Huang, J. Zhou, and P. Carter, "Improved Ultra-Wideband Rectennas Using Hybrid Resistance Compression Technique," *IEEE Trans. Antennas Propag.*, vol. 65, no. 4, pp. 2057-2062, Apr. 2017.

[2] T. W. Barton, J. M. Gordonson, and D. J. Perreault, "Transmission Line Resistance Compression Networks and Applications to Wireless Power Transfer," *IEEE J. Emerg. Sel. Top. Power Electron.*, vol. 3, no. 1, pp. 252-260, Mar. 2015.

[3] S. Dehghani, S. Abbasian, and T. Johnson, "Adjustable Load With Tracking Loop to Improve RF Rectifier Efficiency Under Variable RF Input Power Conditions," *IEEE Trans. Microw. Theory Tech.*, vol. 64, no. 2, pp. 343-352, Feb. 2016.

[4] D. Masotti, A. Costanzo, P. Francia, M. Filippi, and A. Romani, "A Load-Modulated Rectifier for RF Micropower Harvesting With Start-Up Strategies," *IEEE Trans. Microw. Theory Tech.*, vol. 62, no. 4, pp. 994-1004, Apr. 2014.

[5] M. Nick and A. Mortazawi, "Adaptive Input-Power Distribution in Doherty Power Amplifiers for Linearity and Efficiency Enhancement," *IEEE Trans. Microw. Theory Tech.*, vol. 58, no. 11, pp. 2764-2771, Nov. 2010.

[6] S. Yoshida, G. Fukuda, T. Noji, S. Tashiro, Y. Kobayashi, and S. Kawasaki, "Wide power range operable 3-stage S-band microwave rectifier with automatic selector based on input power level," in *2013 IEEE MTT-S International Microwave Symposium Digest (MTT)*, 2013, pp. 1-4.

[7] Y. Y. Xiao, Z. X. Du, and X. Y. Zhang, "High-Efficiency Rectifier with Wide Input Power Range Based on Power Recycling," *IEEE Trans. Circuits Syst. II Express Briefs*, vol. 65, no. 6, pp. 744-748, Jun. 2018.

[8] K. Hamano et al., "Wide dynamic range rectifier circuit with sequential power delivery technique," in *2017 47th European Microwave Conference (EuMC)*, 2017, pp. 1155-1158.

[9] H. Cao, et al., "A novel rectifying circuit with circulator in microwave power transmission," in *2016 IEEE MTT-S International Microwave Workshop Series on Advanced Materials and Processes for RF and THz Applications*, 2016, pp. 1-3.

[10] H. Zhang, Y. Guo, Z. Zhong, and W. Wu, "Cooperative Integration of RF Energy Harvesting and Dedicated WPT for Wireless Sensor Networks," *IEEE Microw. Wirel. Compon. Lett.*, vol. 29, no. 4, pp. 291-293.

[11] X. Y. Zhang and Q.-W. Lin, "High-efficiency rectifier with extended input power range based on two parallel sub-rectifying circuits," in *2015 IEEE International Wireless Symposium*, 2015, pp. 1-4.

[12] M. Huang et al., "Single- and Dual-Band RF Rectifiers with Extended Input Power Range Using Automatic Impedance Transforming," *IEEE Trans. Microw. Theory Tech.*, vol. 67, no. 5, pp. 1974-1984, May 2019.

[13] X. Wang, S. Abdelnasser, and A. Mortazawi, "A 26 dB wide dynamic range rectifier array employing three rectifying devices," in *2017 47th European Microwave Conference*, 2017, pp. 93-96.

[14] X. Wang and A. Mortazawi, "Rectifier Array With Adaptive Power Distribution for Wide Dynamic Range RF-DC Conversion," *IEEE Trans. Microw. Theory Tech.*, vol. 67, no. 1, pp. 392-401, Jan. 2019.

[15] S. Y. Zheng, S. H. Wang, K. W. Leung, W. S. Chan, and M. H. Xia, "A High-Efficiency Rectifier With Ultra-Wide Input Power Range Based on Cooperative Structure," *IEEE Trans. Microw. Theory Tech.*, pp. 1-10, 2019.

[16] C.-J. Li and T.-C. Lee, "2.4-GHz High-Efficiency Adaptive Power," *IEEE Trans. Very Large Scale Integr. VLSI Syst.*, vol. 22, no. 2, pp. 434-438, Feb. 2014.

[17] Z. Liu, Z. Zhong and Y. Guo, "Enhanced Dual-Band Ambient RF Energy Harvesting With Ultra-Wide Power Range," in *IEEE Microw. Wirel. Compon. Lett.*, vol. 25, no. 9, pp. 630-632, Sept. 2015, Sept. 2015.

[18] Z. Liu, Z. Zhong and Y. Guo, "A Reconfigurable Diode Topology for Wireless Power Transfer With a Wide Power Range," in *IEEE Microw. Wirel. Compon. Lett.* vol. 26, no. 10, pp. 846-848, Oct.2016.